Science of the Total Environment 904 (2023) 166891

Contents lists available at ScienceDirect

Science of the Total Environment

journal homepage: www.elsevier.com/locate/scitotenv

Risk assessment for hurricane-induced pluvial flooding in urban areas using a GIS-based multi-criteria approach: A case study of Hurricane Harvey in Houston, USA

Dianyu Feng *, Xiaogang Shi, Fabrice G. Renaud

University of Glasgow, School of Interdisciplinary Studies, Dumfries Campus, Rutherford/McCowan Building, Dumfries DG1 4ZL, United Kingdom

HIGHLIGHTS

- Few risk assessment studies focus on urban social-ecological systems (SES).
- An urban SES flood risk assessment framework with an indicator list was developed.
- Different weighting methods led to slightly different risk profiles.
- The risk maps have a degree of correspondence with recorded flood damages.

GRAPHICAL ABSTRACT

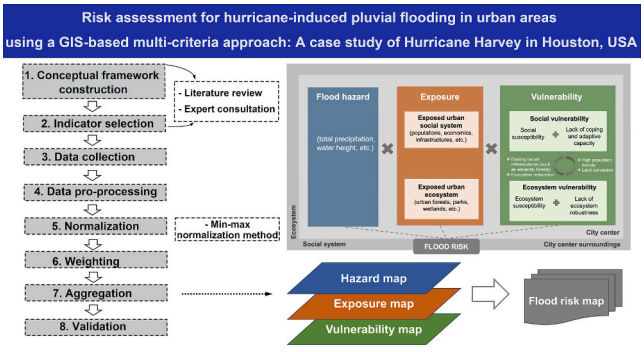

ARTICLE INFO

Editor: Fernando A.L. Pacheco

Keywords:
Extreme weather
Flood risk assessment
Indicator-based method
Social-ecological systems
Urban areas
Houston

ABSTRACT

As one of the most destructive nature hazards, hurricane-induced flooding generates serious adverse impacts on populations, infrastructure, and the environment globally. In urban areas, complex characteristics such as high population and infrastructure densities increase flood disaster risks. Consequently, the assessment of flood risks is becoming increasingly important for understanding potential impacts on an urban area and proposing disaster risk mitigation strategies. After conducting a comprehensive literature review, this study finds that most urban flood risk assessments often overlook urban ecosystem elements, focusing more on social and economic aspects. Hence, the role of urban ecosystems cannot be fully understood. To address this gap, this study proposes a social-ecological systems (SES) flood risk assessment framework for urban areas. Based on this framework, a comprehensive list of indicators collected through a literature review is provided for urban flood risk assessments. A comparative study of flood risk during Hurricane Harvey (2017) in Houston, Texas, USA, is carried out using the improved analytic hierarchy process (IAHP) weighting method and the equal weighting method for indicator weighting. Results are then compared with the damage data of Hurricane Harvey published by the U.S. Federal Emergency Management Agency (FEMA). The analysis identifies that the western part of Houston had the highest flood risks, while the center of Houston was at lower flood risk. Comparisons between the results from the IAHP and equal weighting methods show that the latter produces a broader range of high flood risk areas than the former. This study also highlights the role of urban ecosystems in mitigating flood risks and

* Corresponding author.
E-mail addresses: 2357431f@student.gla.ac.uk (D. Feng), John.Shi@glasgow.ac.uk (X. Shi), Fabrice.Renaud@glasgow.ac.uk (F.G. Renaud).

https://doi.org/10.1016/j.scitotenv.2023.166891
Received 27 June 2023; Received in revised form 23 August 2023; Accepted 5 September 2023
Available online 6 September 2023

advocates for more holistic, social-ecological assessments of flood risk. Such assessments could utilize the proposed framework and the indicator list but contextualize these to the specific urban area's contexts being investigated.

1. Introduction

Flooding is a global issue that affects communities worldwide, causing significant damage to property, infrastructure, and loss of human life (Yildirim and Demir, 2022). According to the Emergency Event Database (Centre for Research on the Epidemiology of Disasters [CRED], 2023), between 2002 and 2021, floods caused an average of approximately 5195 deaths and $41.6 billion in damages per year. Among all types of flooding, hurricane-associated flooding is particularly devastating. The dramatic impacts caused by hurricane season (Hurricanes Harvey, Irma, and Maria) across large areas of the Caribbean, Florida, Georgia, South Carolina, and Texas, USA, in 2017 serves as a reminder that rainfall and flooding can cause substantial damage losses on individuals and society at large. The Hurricane Harvey-related flooding led to the inundation of more than 300,000 infrastructures, and approximately half a million vehicles were impacted. This event not only displaced thousands of people but also caused over $125 billion in economic losses (Blake and Zelinsky, 2018). Hurricanes Irma and Maria-related flooding also caused extensive damage to people, infrastructures, and the local environment of several states in the USA, especially Florida (Cangialosi et al., 2021; Pasch et al., 2023). Furthermore, a study of 28 hurricanes during the 2001–2014 period found that about two-thirds of the residential flood insurance claims were related to freshwater flooding (induced by heavy rain) (Czajkowski et al., 2017), highlighting the severe impacts of the hurricane-related flooding.

In the urban context, hurricane-associated catastrophic rainfall can easily overwhelm the urban drainage system in a very short time (Huang et al., 2020). A high percentage of infrastructures in urban areas prevents water from infiltrating into the soil (Fletcher et al., 2013; Liu et al., 2014). While parks and other open spaces can accommodate floodwater from normal storm events (Liu, 2014; Zimmermann et al., 2016), they are insufficient during extreme rainfall events. A number of studies suggest that flood risk is likely to increase in the future (Tabari, 2020; Wasko and Sharma, 2017). This is primarily due to increased population density in high flood-prone regions globally. Currently, 56 % of the world's population lives in urban areas, and the world's urban population is projected to increase by a factor of 1.5, reaching an estimated total of 6 billion by 2045 (World Bank, 2023). In the context of flooding, a dense population in urban areas means potentially more exposed people to flood hazards (Tellman et al., 2021). In addition, the conversions of green areas and agricultural land to impervious surfaces also have severe impacts on urban biodiversity and ecosystem services (Hanh Nguyen et al., 2023). In recent years, the growing awareness that human and their surrounding environment are integrated has led to an increasing number of studies focusing on social-ecological systems (SES) in urban areas (Herath and Wijesekera, 2019). Finally, extreme rainfall is expected to intensify with global warming (Knutson et al., 2021; Li et al., 2023). A study on the Gulf of Mexico region, USA, shows the increase in maximum inundation extent will be 11.0 % (2050s) and 19.5 % (2090s) per degree Celsius increase in Mean Surface Temperature (Li et al., 2023).

Being hotspots of ongoing and projected global change impact, including population growth and economic development, the state of urban areas has great significance for sustainable development, generally speaking. Urban areas are key to achieving the Sustainable Development Goals (SDGs), especially SDG 11 (Sustainable Cities and Communities), SDG 13 (Climate Action) and SDG 15 (Life on Land) (United Nations, 2015). Urban areas are, of course, highly relevant to achieving the targets of the Sendai Framework for Disaster Risk Reduction (SFDRR) 2015–2030, such as reducing global disaster mortality, reducing the number of affected people globally and reducing disaster damage to critical infrastructure and disruption of essential services by 2030 (UNDRR, 2015). Flood risk-informed planning of future development, as well as targeted disaster risk reduction (DRR) and adaptation strategies, will be not only important but also essential in urban areas in the coming years. This requires spatially explicit, integrated information on the flood risks in urban areas in an integrative manner. In this context, a comprehensive flood risk assessment can provide important information for flood risk management and planning in urban areas (Meyer et al., 2009; Schanze, 2006).

By addressing the challenges described above, an indicator-based methodology for flood risk assessment in an urban SES setting was developed and piloted in Houston City, USA. The case study selected for this research is Hurricane Harvey, an extreme hurricane event. According to research conducted by Zhang et al. (2018), urbanization has increased the probability of such extreme flooding events by a factor of nearly 21 times. Hence, the flood risk assessment for this representative event can provide important information not only for Houston but also for other regions facing similar threats. The conceptual framework with a list of comprehensive indicators can be applied generically as an initial step before conducting flood risk assessments in specific regions. Overall, the objectives of this study are: (i) Conduct a comprehensive literature review to understand the current state of urban flood risk assessments; (ii) develop a flood risk assessment framework as well as an indicator list for urban SES; (iii) apply the proposed SES flood risk assessment framework to a real-world scenario and compare the results of two different weighting methods; (iv) carry out a preliminary validation by comparing the generated flood risk maps with actual damage data from Hurricane Harvey as published by the U.S. Federal Emergency Management Agency (FEMA).

2. Study area and methods

2.1. Study area

Houston is the largest city in Harris County and the fourth largest city in the U.S., with a total area of 1722 km^2 and a population of about 2.3 million (City of Houston, 2014). Fig. 1 shows the position and elevation of Houston. Due to the proximity to the Gulf of Mexico, Houston is one of the most exposed urban areas globally with respect to hurricanes (Chakraborty et al., 2018). Each year, during the rainy season from April to October, Houston is threatened by flooding from heavy rainfall. The flat terrain and rapid urbanization have both worsened flooding in this area (Li et al., 2019).

Hurricane Harvey struck Texas on August 25th, 2017, and induced catastrophic flooding in the region. The creeks and bayous across the city reached the highest water levels on record. Nine out of nineteen official river gauges in Harris County recorded all-time high flood stages (Blake and Zelinsky, 2018). FEMA (2017) reported that around 30,000 water rescues were recorded during Hurricane Harvey. Moreover, 36 Harvey-related deaths were recorded in the Houston metropolitan area (FEMA, 2017). Therefore, this event had significant social, economic, and physical impacts.

2.2. Risk assessment and conceptual frameworks

2.2.1. Conceptual frameworks used in urban flood risk assessments

To understand the conceptual frameworks and indicators used in previous urban flooding risk assessment studies, a literature review was carried out, sourcing papers through Scopus. Detailed information about

the literature review process can be found in Appendix B. Through the search, Scopus returned 4333 records. A total of 120 papers were identified for review after sequentially screening the titles, abstracts, and main texts (the specific criteria used in each selection process can be found in Appendix B). This study mainly focuses on pluvial urban flooding, but flooding can be from various sources and processes, such as storm surge-induced coastal flooding. To ensure the literature review was comprehensive, papers which addressed different types of flooding in urban areas were included.

Understanding disaster risk and its components is the first step in the process of flood risk assessment. Due to the differences in research contexts, the definition of risk and conceptual frameworks differ between studies. Table A.1 in Appendix A provides a summary of risk equations, the definitions of risk, and its components adopted in the reviewed studies. Some researchers used a traditional definition of risk in the context of natural sciences, engineering, and economics. In this context, risk can be conceptualized as the probability of adverse consequences (Scheuer et al., 2011). Eq. (A.1) shows that risk is composed of two components: occurrence of the hazard and the consequence of the manifestation of the hazard. Based on this equation, the UK Institution of Civil Engineers proposed the Source-Pathway-Receptor-Consequence (SPRC) model to identify the risk of flooding and erosion (Sayers et al., 2002). By using the SPRC model, Kandilioti and Makropoulos (2012) assessed the flood risk in the central and most urban regions of Greater Athens areas. The SPRC model helps to illustrate the theoretical link between the flood events (sources) through discharge and flooding (pathways) to the impacts on elements at risk (receptors) and their consequences (Kandilioti and Makropoulos, 2012). Yan et al. (2016) also used the SPRC model as the conceptual basis to assess the possible impacts of projected flood risks caused by sea-level rise and storm surges (sources) in Shanghai, China. The advantage of this model is that the whole process can be understood in an intuitive way, but the use of the SPRC model is often poorly defined and unclear, making it hard to assess flood risks accurately (Narayan et al., 2012).

In the context of disaster risk science, risk is characterized as a function of hazard and vulnerability (see Eq. (A.2) in Appendix A) and can be calculated by simply multiplying the two factors (Chakraborty and Mukhopadhyay, 2019; Eini et al., 2020; Percival et al., 2019; Vlad and Nedelcu, 2011; Waghwala and Agnihotri, 2019), and exposure is normally embedded in "vulnerability". Based on this equation, Percival et al. (2019) constructed a model that assessed the coastal flood vulnerability and risk for urban communities in Portsmouth, UK. The results of vulnerability and hazard were calculated separately, and then combined to assess the final risk. Three elements of vulnerability were considered in their study, physical vulnerability, social-economic vulnerability, and resilience. Using a similar approach, Waghwala and Agnihotri (2019) assessed the impacts of urbanization on flood risk in Surat City, India, by comparing the flood risks in 1968 and 2006.

In some studies, exposure was added separately to compute the risk, with the risk being a function of hazard, vulnerability, and exposure (see Eq. (A.3) in Appendix A) (Rana and Routray, 2018; UNDRR, 2019; Intergovernmental Panel on Climate Change [IPCC], 2022). Based on

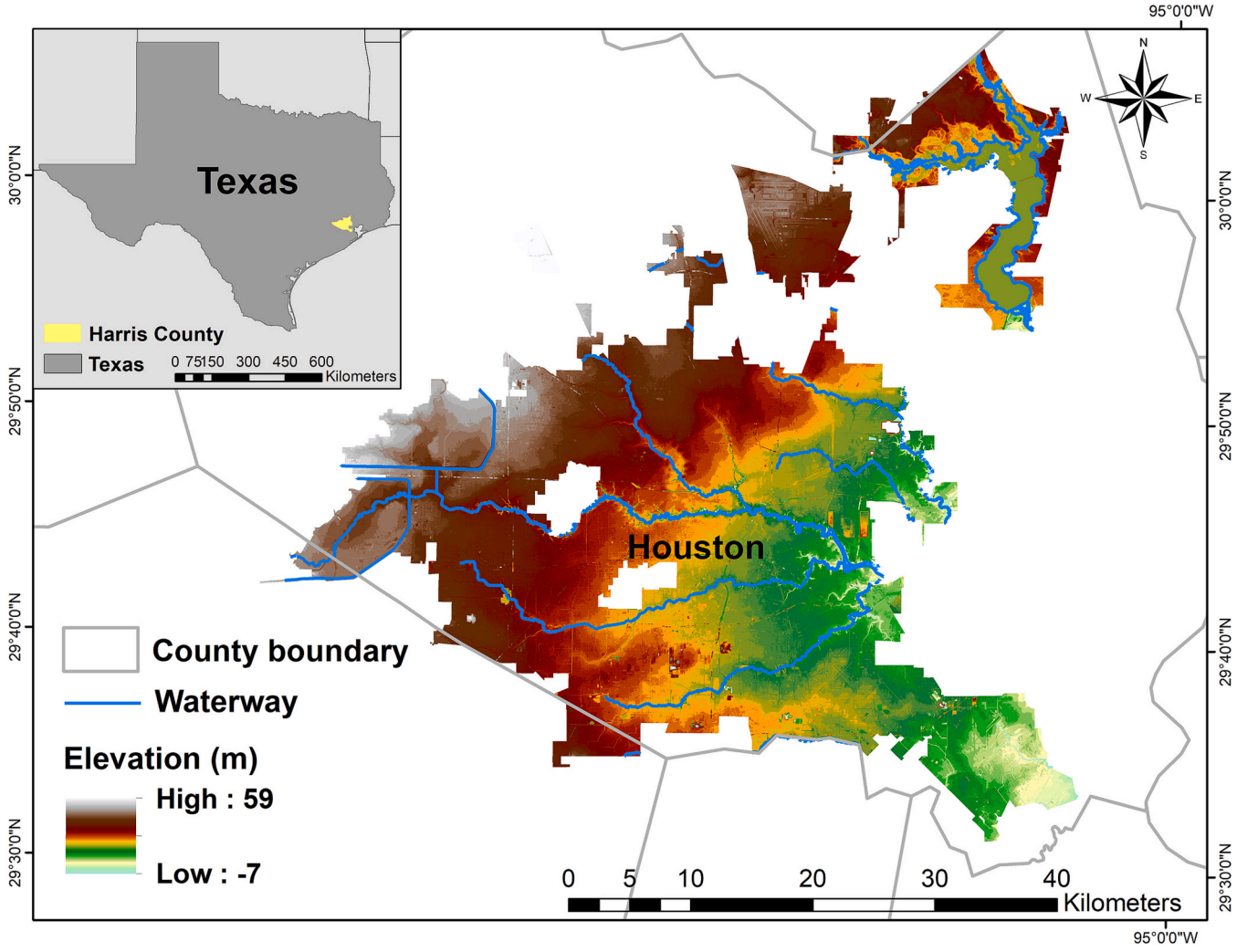

Fig. 1. Location and the Digital Elevation Model (DEM) map of Houston (own figure, data from United States Geological Survey, 2011).

this equation, a conceptual framework for flood risk assessment in large urban agglomerations in Santiago de Chile was proposed by Müller (2013). Three dimensions of vulnerability were considered in this conceptual framework: physical, economic, and social vulnerability (Müller, 2013). Müller (2013) justified this approach by the fact that the natural environment and economic activities were not considered because the study area is residential.

Since vulnerability is one of the main components of risk, the literature review also included studies focusing on flood vulnerability assessment. A summary of equations and the definitions for vulnerability assessments are presented in Table A.2 in Appendix A. In the reviewed flood vulnerability assessment studies, exposure is one of the components of vulnerability and vulnerability is mainly represented by three components: exposure, susceptibility, and resilience. The Methods for the Improvement of Vulnerability Assessment in Europe (MOVE) framework was proposed by Birkmann et al. (2013) to address vulnerability and risk to natural hazards. In this framework, various dimensions of risk management and climate change adaptation can be assessed at different times and spaces (Birkmann et al., 2013). The MOVE framework is not hazard-specific and can therefore be used in various contexts. Kablan et al. (2017) assessed the social vulnerability in Ivory Coast to flooding using the MOVE framework. In their study, the framework worked as the conceptual tool for guiding indicator selection and social vulnerability assessment at the local level. Thirteen indicators that consider the social, physical and ecological dimensions of vulnerability were used in their study. However, only one ecological indicator: Vegetation cover per sub-district (%), was considered. Balica et al. (2012) modified a framework for coastal flood vulnerability assessment at the city level based on Eq. (A.4) in Appendix A. In their study, nineteen indicators were selected and applied to nine coastal cities for flood vulnerability assessment. Kamat (2019) analyzed urban flood vulnerability in Bhopal, India, by using Eq. (A.5) (Appendix A). A total of sixteen physical and socio-economic indicators were selected in this study.

The review revealed a few gaps in previous research. Firstly, many reviewed studies did not define the risk and its components clearly. This can lead to setting ambiguous objectives for flood risk assessments. A clear conceptual framework is required to address complex urban characteristics. Secondly, the reviewed studies rarely consider all risk domains – social, economic, ecological, and physical – that are potentially at risk from flooding. Most previous flood risk studies examined social-economic vulnerability and risk, while ecological elements were not well characterized. Even though some papers used ecological-related indicators, the number of such indicators in the assessments was very limited. In the context of urbanization, the ecosystem of urban areas plays an important role in disaster risk reduction, especially with the rise of nature-based solutions (NBS) in urban areas (Kablan et al., 2017). According to a report conducted by the European Commission (EC) (2021), urban areas account for less than 4 % of the land around the world, but almost all the funded NBS-related projects by the EC before 2018 focused on urban and/or coastal areas. NBS has been described as solutions that can be combined with other engineered measures (e.g., green and grey measures) to address urban disaster risk reduction objectives (Depietri and McPhearson, 2017). In this context, this study aims to construct a more comprehensive conceptual framework for reflecting the flood risk in the SES urban settings.

2.2.2. *Conceptual framework adopted in this study*

Based on the above, a conceptual framework was developed for urban flood risk assessment. It builds on and extends a multi-step, iterative methodology for index construction and risk assessment. The overall structure is based on the Delta-SES framework developed by Sebesvari et al. (2016) (Fig. 2), which has also been used in other studies and contexts (Peng et al., 2023; Shah et al., 2020). The departure from the Delta-SES framework is that this study only considers flood hazard (as opposed to a multi-hazard context), and the basic geographical boundary of risk assessment is at the city level. Urban characteristics are therefore considered explicitly.

In this framework, flood risk is conceptualized based on three components: the characteristics of flood hazard, the level of exposure of urban SES, and the vulnerability of the exposed SES system. The equation is shown in Eq. (A.3) in Appendix A (UNDRR, 2019; IPCC, 2022).

We followed definitions of risk and its components as provided by IPCC (2022): Risk is conceptualized as the potential adverse consequences for human and ecological systems. Hazard refers to the possible

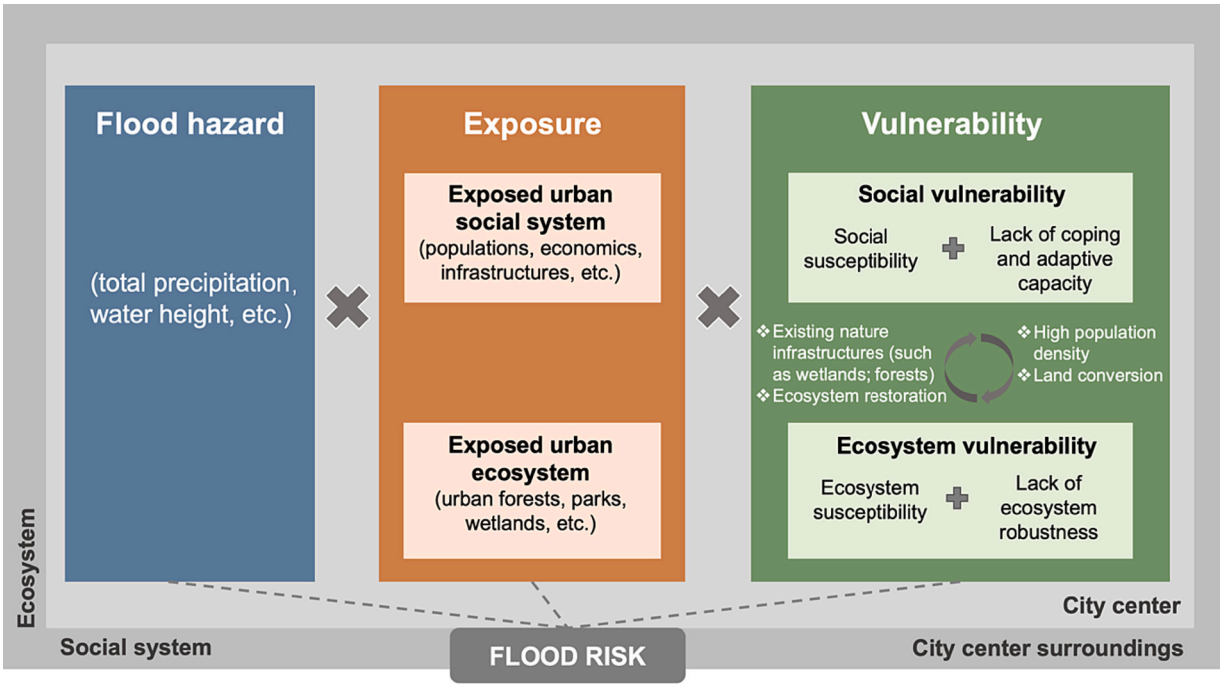

Fig. 2. The urban SES framework for flood risk assessment.
Modified from Sebesvari et al. (2016) and IPCC (2014).

occurrence of natural or human-induced events that could negatively affect vulnerable elements. Exposure refers to the presence of humans, livelihoods, species or ecosystems, infrastructure, or economic, social, or cultural assets in places and settings that could be adversely affected. Vulnerability refers to the inherent tendency to be negatively affected and includes a variety of elements, including sensitivity or susceptibility to damage and lack of capacity to cope and adapt.

The proposed framework views flood risk as related to a particular city where there are interactions between the urban social system and the urban ecosystem. Exposure to both the social system and ecosystems is considered. In urban areas, population, infrastructures, and economic activities exposed to floods can be seen as important elements of social exposure. Ecosystem exposure mainly includes exposed urban forests, wetlands, parks, and lakes. Vulnerability is divided into social vulnerability and ecosystem vulnerability. There are four sub-components: social susceptibility, lack of coping and adaptive capacity, ecosystem susceptibility and lack of ecosystem robustness (Sebesvari et al., 2016). Susceptibility indicates the relative damageability of the population and property during flood hazards (Balica et al., 2009). It is closely related to system characteristics, including the social context of flood damage (Balica et al., 2009), such as the population's age distribution, health condition, cultural background, and education level. Coping and adaptive capacity refers to the ability of individuals and communities to effectively manage and respond to the risks and impacts of nature hazards (e.g., available response measures) and their learning aspects (e.g., existing precautionary measures). This can be due to a variety of factors, such as poverty, inadequate infrastructure, and limited access to resources and services. Ecosystem robustness means an ecological system's capacity to resist disturbance (Damm, 2010). Overall, the urban SES framework should be understood as a complex system with diverse characteristics. For practical reasons, it can be modified to suit the specific conditions of other cities worldwide beyond Houston.

2.3. Indicators and data collection

2.3.1. Indicators used in urban flood risk assessments

The proposed framework (Fig. 2) provides a conceptual structure so that all 117 indicators collected from the reviewed articles could be assigned to the corresponding risk components and sub-components: flood hazard, ecosystem exposure, social system exposure, ecosystem vulnerability and social system vulnerability (see Appendix C for all the indicators).

The hazard was characterized through indicators related to rainfall characteristics. The review showed that flood-related indicators typically aimed to show the influences of heavy rainfall on surface water, such as 'water height' and 'streamflow'. For coastal cities, indicators like 'Height of storm surges' and 'Tidal range' inform on coastal-type flood hazards. For the exposure part, indicators on the presence of population, economic activities and infrastructures have been used frequently in the reviewed studies. Furthermore, the characteristics of local populations, such as age, gender and health conditions, are the most frequently used indicators in vulnerability assessment.

Comparing the number of indicators of the social system and ecosystem in the exposure and vulnerability categories, respectively, the number of indicators for social exposure (23) is greater than ecosystem exposure (6), and the number of indicators for social vulnerability (58) is greater than ecosystem vulnerability (13). This disparity may be due to the social dimensions of exposure and vulnerability being more varied and complex in urban contexts. Other research in different contexts, such as Sebesvari et al. (2016), Hagenlocher et al. (2018) and Shah et al. (2020), also came to similar findings. This consistency across research further underscores the trend and suggests the need for potential readjustment to achieve a more balanced understanding of both social and ecological exposure and vulnerability.

2.3.2. Indicator selection in this study

The indicators for urban flood risk assessment were identified through a combination of the outcomes of the literature review and a questionnaire survey. Six researchers with expertise in natural hazards were invited to fill out an online questionnaire to select indicators for urban flood risk assessment in Houston (see Appendix H for the questionnaire). Among the six researchers, four specialized in natural hazard risk assessment, and two specialized in hydrological modelling and hydro-meteorological risk assessment. Their research backgrounds equipped them with the necessary knowledge to make valuable contributions to urban flood risk assessment studies. The survey received the ethical clearance from the College of Social Sciences, University of Glasgow. The selected indicators through this survey were organized in an indicator list, which is categorized into three main risk components: hazard, exposure and vulnerability (Fig. 3).

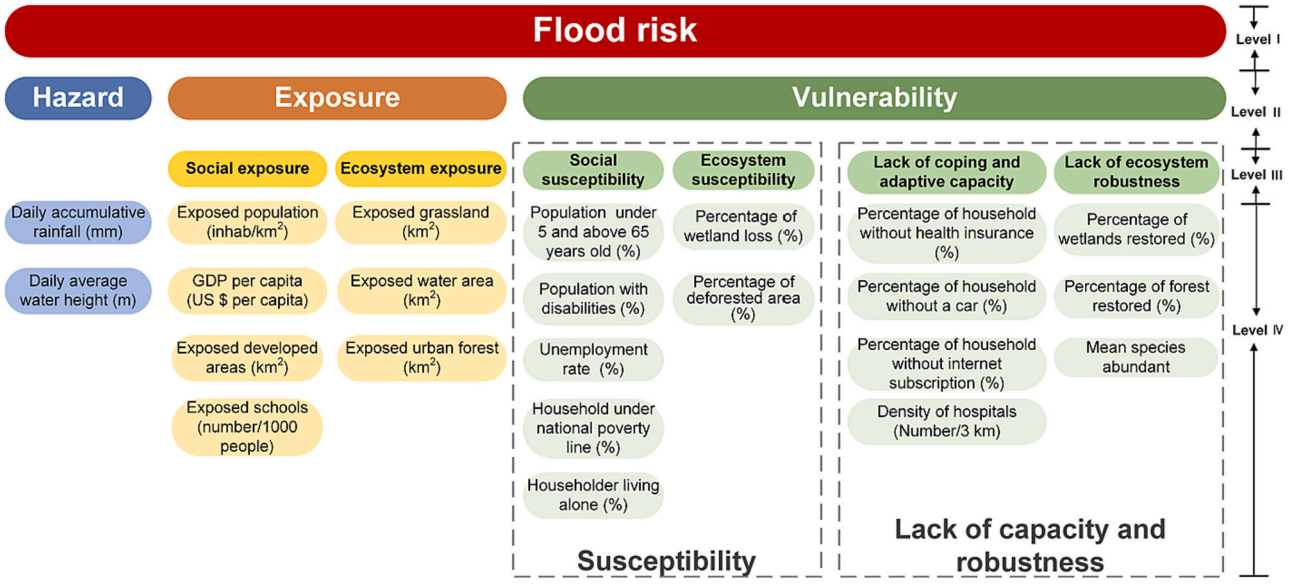

Fig. 3. Selected indicators for each risk component (Level I means the final risk level; Level II means the three risk components, Level III means the subcomponents of risk; Level IV means the indicator level).

2.3.3. Data collection and pre-processing

Data for the quantification of the indicators were collected from different sources (as shown in Table A.3 in Appendix A): (a) time series observations (e.g. daily accumulative precipitation and daily average water height); (b) raster (e.g. land cover at a 30 m resolution); (c) vectors (e.g. city boundary and river network data); (d) official documents (e.g. data from the U.S. Census 2017 American Community Survey).

Except for data from printed documents, all the data were processed using ArcGIS version 10.8. All raster datasets were projected, resampled to a 30 m grid cell, and clipped to the study area so all input grids were accurately overlaid with the identical projection, cell size and map extent. Appendix D provides an overview of the datasets and data processing steps.

Data pre-processing followed the steps of missing data analysis, outlier detection and treatment and multicollinearity detection (Anderson et al., 2021) (see Appendix E for detailed rules and the results for each step). These steps were conducted in SPSS (IBM SPSS Statistics). The final set of indicators and values were standardized using linear min-max normalization (see Eq. (1)), creating indicator data series with a mean of 0 and standard deviation of 1.

$$x_{scaled} = \frac{x - x_{min}}{x_{max} - x_{min}} \tag{1}$$

2.4. Weighting methods

2.4.1. Weighting methods used in published urban flood risk assessments

Several multi-criteria integrated procedures can be used to weight the indicators in the flood risk assessment process, such as equal weight, analytic hierarchy process (AHP) and outranking. Each method has specific characteristics, and researchers can select suitable approaches based on the context of their study areas. The review revealed that the most frequently used weighting methods are AHP (36 reviewed articles) and the equal weighting method (14 reviewed articles). Some papers stated that the weights for each component were obtained by expert judgments without further explanation. Many papers did not mention the specific weighting method used in their studies.

AHP is a structured technique for analyzing complex problems, and it is normally used with GIS in flood risk assessments. This combination has been proven to be an effective tool for combing indicators to support flood risk assessment (Rincón et al., 2018; Zhang et al., 2020). Assigning equal weight to the indicators is another common weighting method in the reviewed articles. Scheuer et al. (2011) assigned equal weight to economic, social, and ecological risk in their studies. Yilmaz et al. (2015) also assigned equal weights to the flood vulnerability indicators in their studies. Except for the two weighting methods mentioned above, the rating method was also adopted in some reviewed articles. Yeganeh and Sabri (2014) used the rating method to weigh the flood vulnerability criteria. Based on the rating weighting method, Elboshy et al. (2019) assigned weight for vulnerability indicators by collecting questionnaires from experts and the final weight was calculated by giving an equivalent percentage to each averaged rating.

2.4.2. Weighting method used in this study

This study selected two weighting methods to assign weight to each indicator: equal weight and AHP methods. By using equal weight, each indicator is assigned the same weight in the calculation process, which is equally influential across the study area. Compared with the equal weight, the AHP method requires the participation of experts to gather opinions and preferences on the selected indicators. This method has several weaknesses, such as the inconsistency of the comparison matrix and the complex procedure associated with constructing the pairwise matrix (Li et al., 2013). To address these problems, an improved analytic hierarchy process (IAHP) method is adopted and implemented to assign the weights to the indicators in this study. The IAHP method can simplify the process of judgment matrix construction and ensure the consistency of the judgment matrix (Zhang et al., 2020). The specific steps are to: a) construct a hierarchical structure for indicators, b) sort the elements at each level (see Fig. 3), c) assign the values to the indicators/indexes by linear interpolation, and d) calculate the weight by constructing a matrix.

In order to sort the indicators, an online questionnaire was designed for weight assignment. Seven experts who have knowledge about flood hazards in Houston were invited to fill out this questionnaire. After receiving feedback from the experts, the judgment matrix $[a_{ij}]$ (see Eq. (2)) is used to determine the relative importance of factor a_i to factor a_j based on the expert opinion.

$$aij = \begin{bmatrix} a_{11} & \cdots & a_{1m} \\ \vdots & \ddots & \vdots \\ a_{m1} & \cdots & a_{mm} \end{bmatrix} \tag{2}$$

The matrix should meet the following conditions (Eq. (3)):

$$\begin{cases} \sum a_{ij} = 1 \\ a_{ij} = 1/a_{ji} \end{cases} \tag{3}$$

Then, the consistency of the judgment matrix can be validated by the value of the consistency ratio (CR). CR can be computed by Eq. (4) in Microsoft Excel software, where CI is the Consistency Ratio, and RI is the Random Consistency Index. A CR value of less than 0.1 means successful execution of the test, while a higher value indicates that the comparison matrix needs to be reconstructed (Lyu et al., 2018).

$$CR = CI/RI \tag{4}$$

Fig. 4 shows the weight assignment in this study. The detailed calculation process can be found in Appendix G. For the hazard, Daily average water height was deemed more important than Daily accumulative precipitation. Due to the urban context, social-related indicators (both exposure and vulnerability) were assigned more weight in the final risk calculation. This was particularly true for the exposure part, where social exposure accounts for 84 % and ecosystem exposure accounts for 16 % of total SES exposure. Indicator SE1 (Exposed population) accounts for the largest proportion (50 %) of all indicators under the exposure component. In the vulnerability part, there are three indicators that are more significant than the other indicators: Population under 5 and above 65 years old, Population with disabilities and Percentage of wetland loss.

After calculating the weight for each indicator, the indicators within one risk component were aggregated using Eq. (5). There are three layers in the indicator framework (see Fig. 3), the aggregation process was taken from the lower layer then to the higher layer.

$$R = \sum_{i=1}^{n} (w_i * x_i) \tag{5}$$

Ultimately, hazard, exposure and vulnerability were combined to give the flood risk index through multiplicative aggregation. Aggregation of indicators and risk components was carried out in Microsoft Excel 2016, and results were visualized in ArcGIS 10.8. The Janks Natural Breaks Classification Method was used for data clustering in this study, and all indicators are classified into five classes using the 'classified tool' in ArcGIS 10.8.

3. Results and discussions

3.1. Hazard assessment

The hazard index is used to represent the characteristics of flood hazards during Hurricane Harvey, which in turn is represented by two indicators: Daily accumulative precipitation (H1) and Daily average water height (H2). The gage stations, dedicated to recording real-time data for these two indicators, are located across the city. For a comprehensive understanding of their geographical locations, refer to

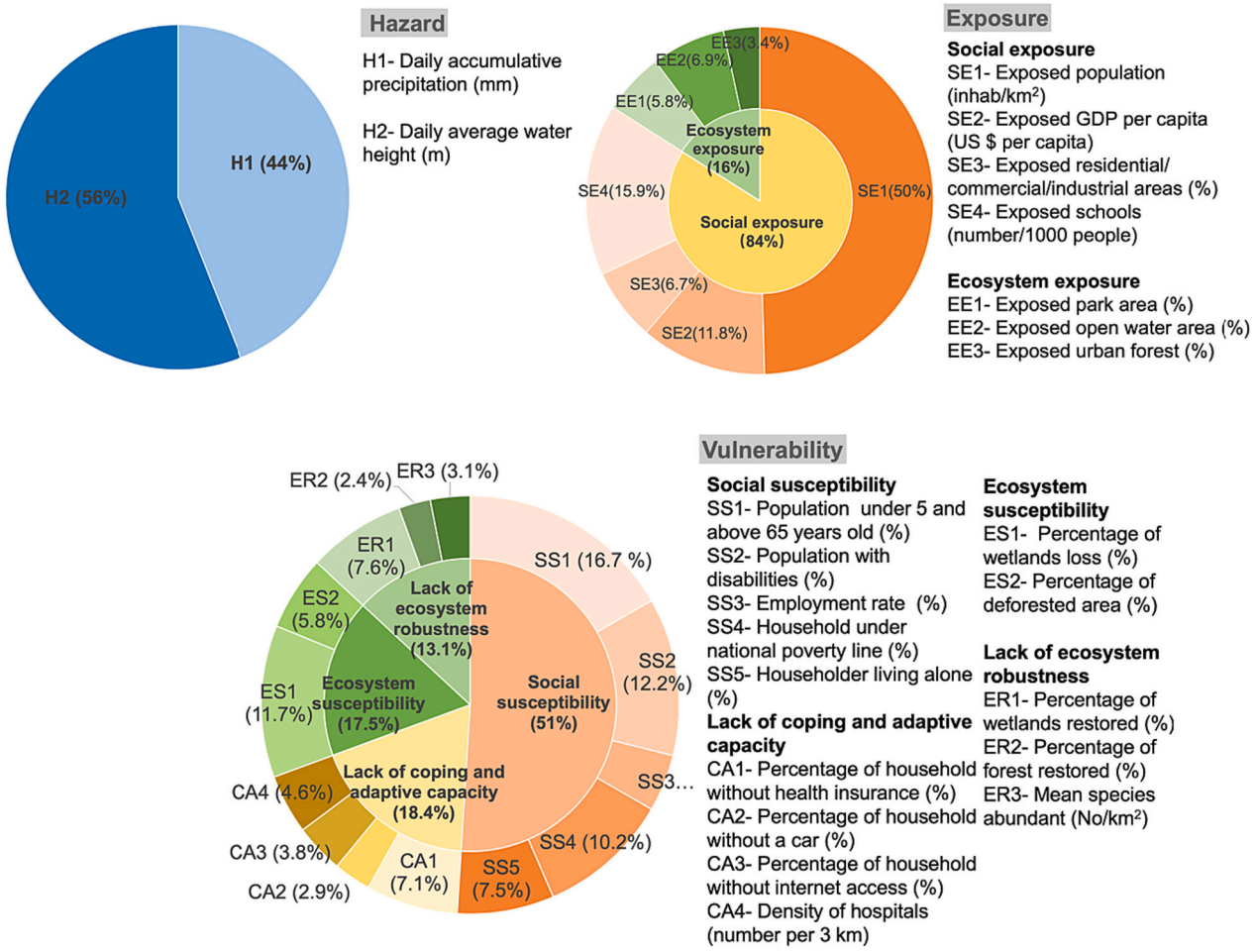

Fig. 4. IAHP weight assignment of each indicator under the Hazard, Exposure and Vulnerability. The selected indicators and their weights are suitable for Houston but may not be relevant for other regions, especially the ecosystem elements. For other cities with different environmental characteristics, the indicators should be tailored accordingly.

Fig. D.2 in Appendix D. Fig. 5(a) shows the hazard score map of 27th August 2017 calculated using the IAHP method. This map can be considered as the maximum flood hazard map throughout Hurricane Harvey. A significant spatial variation in flood hazard level is discernible across the map, with a general decline from northwestern to southeastern Houston. Overall, the northwestern region has a very high level of flood hazard and the southeastern has a relatively lower level of flood hazard. Conversely, the central region reveals the lowest hazard level. To interpret the trends of flood hazard levels throughout the duration of Hurricane Harvey, a heatmap was made, as depicted in Fig. 5(b). This visualization represents the temporal shifts in flood hazard levels across various neighborhoods from August 25th to August 31st, 2017. In the initial stages of the hurricane, the flood hazard of the entire area increased with time, reaching maximum values on the 27th of August. Following this peak, the flood hazard score gradually decreased, reflecting the attenuation of the flood impacts caused by Hurricane Harvey over time.

3.2. Exposure assessment

The Maximum Observed Flooding Map of Hurricane Harvey developed by the Dartmouth Flood Observatory (Brakenridge and Kettner, 2023) was used to calculate the exposure in this study. Fig. 6 shows the social exposure, ecosystem exposure and exposure maps, which were evaluated by the IAHP method. Generally, the spatial distribution of social exposure is predominantly concentrated in the western and southeastern parts of the region, while the spatial distribution of ecosystem exposure is higher in the western and northeastern of Houston. The highest socially exposed areas mainly include a higher living population and a more extensive presence of developed land uses, such as residential, commercial, and industrial zones. Neighborhoods demonstrating very high level of ecosystem exposure, such as neighborhoods 9 and 17 in the west, neighborhood 37 in the southwest, and neighborhoods 43 and 44 in the northeast of Houston, are typically characterized by abundant green areas and open water areas.

Combining the social exposure and ecosystem exposure, the overall SES exposure maps are presented in Fig. 6(c). Of particular note are neighborhoods 9, 17 and 39 in the western, neighborhood 60 in the middle and neighborhoods 53, 54, 56 80 in the east of Houston, which exhibit remarkably elevated exposure levels. The weight assignments for social and ecosystem exposure are respectively 84 % and 16 %. It demonstrates that the overall exposure level is predominantly influenced by social factors. Nevertheless, ecosystem exposure retains a significant role in shaping the final exposure pattern.

3.3. Vulnerability assessment

A disaggregation of vulnerability scores was first conducted by comparing the four vulnerability subcomponents: Social susceptibility, Lack of coping and adaptive capacity, Ecosystem susceptibility and Lack of ecosystem robustness, as shown in Fig. 7(a–d), respectively. For Social susceptibility and Lack of coping and adaptive capacity maps, hotspots

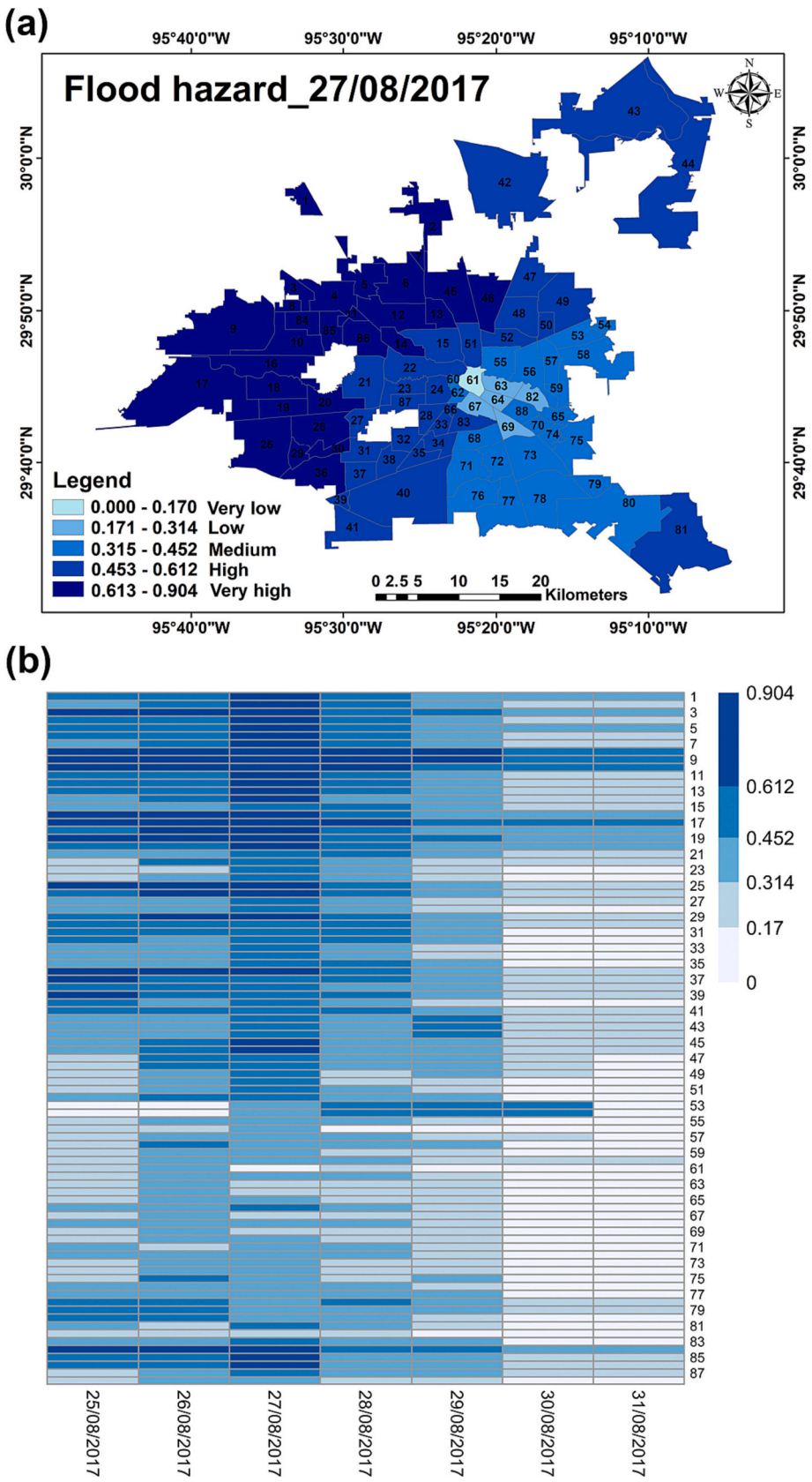

Fig. 5. (a). Flood hazard map using the IAHP method.
(b) Heatmap of flood hazard level from 25th August 2017 to 31st August 2017 using the IAHP method. For the heatmap, the X coordinate represents the date, and the Y coordinate represents the ID of 88 neighborhoods in Houston. Y-axis show only odd-numbered IDs for clarity. In both maps, dark blue tracts correspond to high hazard scores and light blue tracts to low hazard scores.

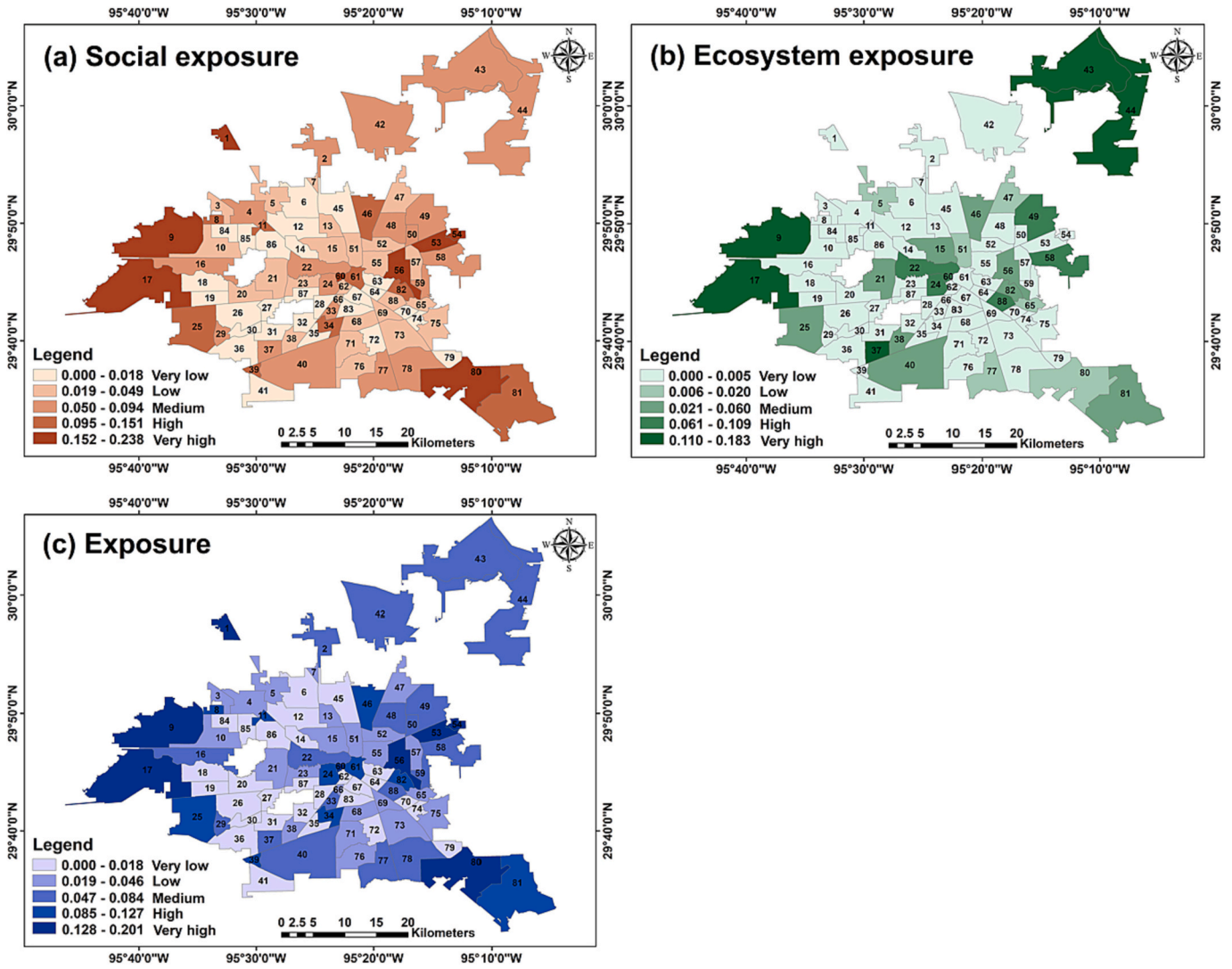

Fig. 6. (a) Social exposure, (b) ecosystem exposure and (c) SES exposure of Houston using the IAHP method. In the maps, darker color tracts correspond to higher exposure scores and lighter color tracts to lower exposure scores.

are mainly located in the eastern region of Houston. As for the maps of Ecosystem Susceptibility, a majority of the neighborhoods exhibit relatively lower scores. Compared with the other three maps, most areas in Houston show a high level of Lack of ecosystem robustness. This is to be expected as this vulnerability component was assessed through merely three indicators, two of which were based on the restoration of natural areas and the remaining one based on biodiversity. In urban areas, all these elements are predicted to have low scores, thereby contributing to a higher level of Lack of ecosystem robustness. Out of 117 indicators shown in Appendix C, only seven indicators are related to Ecosystem robustness, thus making it challenging to comprehensively understand the role of this component very well, especially in light of the burgeoning presence of NBS projects in urban areas.

By combining the subcomponents, social system vulnerability and ecosystem vulnerability maps, as illustrated in Fig. 7(e–f), show several hotspots of very high social vulnerability and ecosystem vulnerability. For example, due to the higher density of vulnerable demographic groups (e.g., aged population and disabled population), several neighborhoods in the east of Houston show higher social vulnerability scores. Similarly, since neighborhoods 19 and 39 have lost about 49 % and 68 % of wetlands, respectively, over the past decade (National Oceanic and Atmospheric Administration [NOAA], 2023), they have very high ecosystem vulnerability. By comparing the maps of social and ecosystem vulnerability, the areas with higher social vulnerability normally have lower ecosystem vulnerability. For example, neighborhood 44, which is Lake Houston area, logically has 'very low-level' social vulnerability but 'medium-level' ecosystem vulnerability.

Flood vulnerability in Houston was then visually interpreted in Fig. 7 (g). A grouping of high vulnerability scores in the northeast of Houston is evident. Comparatively, the central region of Houston is identified as having lower vulnerability relative to other regions. By comparing all figures in Fig. 7, it is evident that social susceptibility is the dominant component contributing to both social and overall SES vulnerability. This can be easily explained by the weight difference, the social susceptibility accounting for 51 % of the total weight, which is the highest among the four vulnerability components. It indicates that social factors are deemed to play a substantial role in the city's vulnerability.

3.4. Risk assessment

The hazard, exposure and vulnerability spatial distribution map layers were combined to obtain integrated risk scores for the region (Fig. 8). Similar to the hazard, heatmaps were made to illustrate the daily fluctuations in relative flood risk levels throughout this period. It is noteworthy that each map employed the same risk range for consistency in comparison. A comparative analysis was conducted to discern the

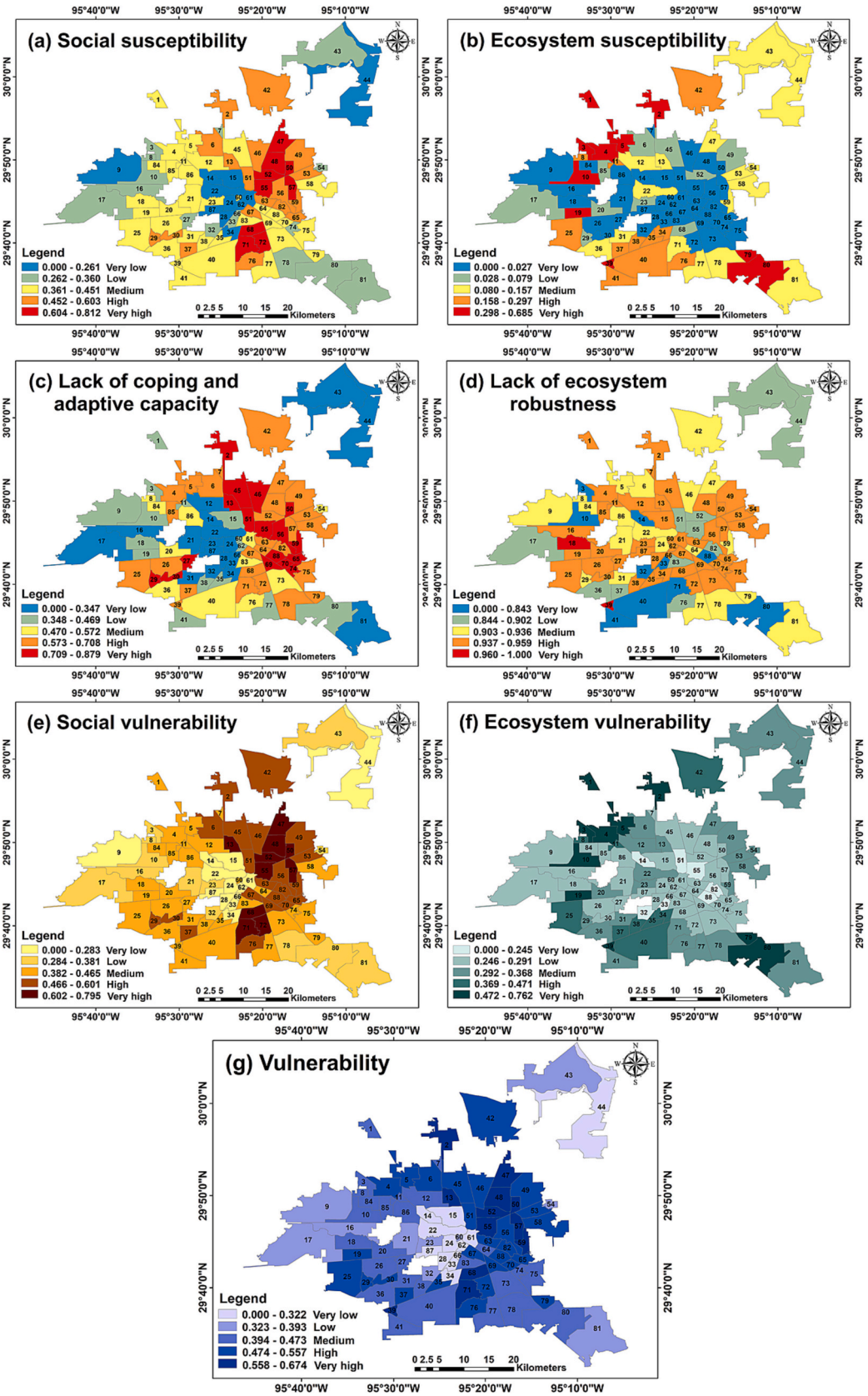

Fig. 7. Maps of (a) social susceptibility, (b) ecosystem susceptibility, (c) lack of coping and adaptive capacity, (d) lack of ecosystem robustness, (e) social vulnerability, (f) ecosystem vulnerability and (g) vulnerability in Houston by using the IAHP method. For the four vulnerability components' maps, red tracts correspond to high vulnerability and blue tracts to low vulnerability. For social vulnerability, ecosystem vulnerability and vulnerability maps, darker color means higher vulnerability.

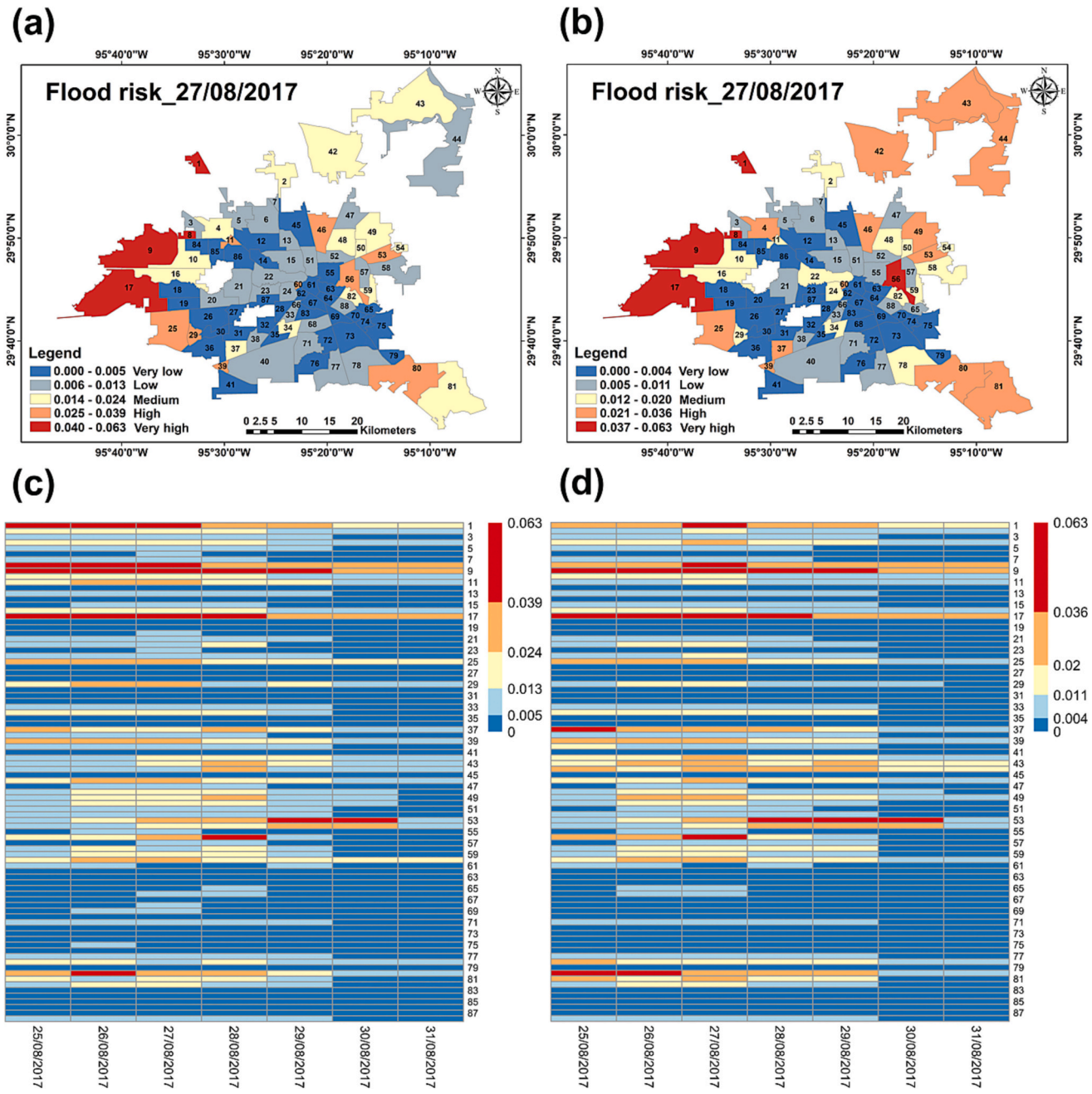

Fig. 8. Maps of (a) flood risks of Houston on 27th August 2017 using the IAHP method, (b) flood risks of Houston on 27th August 2017 using the equal weighting method, (c) heatmap of flood risk level from 25th August 2017 to 31st August 2017 using the IAHP method, (d) heatmap of flood risk level from 25th August 2017 to 31st August 2017 using the equal weighting method. Red tracts correspond to high-risk scores and blue tracts to low-risk scores. For (c) and (d), the X coordinate represents the date, and the Y coordinate represents the ID of 88 neighborhoods in Houston. Y-axis labels show only odd-numbered IDs for clarity.

differences in risk levels generated by two weighting methods. Like the trend of flood hazard scores, the flood risk levels of several neighborhoods increased during the first three days and reached the highest risk levels on 27th August 2017 for both methods. On this date, both methods identified four neighborhoods (No. 1, 8, 9 and 17) have very high-level flood risk. Flood risks then decrease gradually during the following four days. After comparing the heatmaps generated by the two weighting methods, it became evident that the equal weighting method yields a higher risk level for several neighborhoods.

To further compare the results of the two weighting methods, a series of figures (see Fig. A.4 in Appendix A) were created to determine what percentage of neighborhoods fell in each of the five risk classes. For the initial assessment conducted on 25th August 2017, both the IAHP and the equal weighting method yielded similar distributions across the risk levels, with the majority of neighborhoods falling within the "very low" to "low" risk categories. A difference was observed in the "medium" and "high" level, where the IAHP attributed a slightly higher percentage to "medium" risk (0.14) compared to the equal weighting method (0.10), and vice versa for the "high" risk category.

As the week proceeded, discrepancies between the IAHP and equal weighting methods became more apparent. The equal weight consistently classified a higher proportion of neighborhoods under 'medium' and 'high' risk levels than the IAHP method, particularly on 26th August 2017 and 27th August 2017. The difference between the two methods diminished slightly on 29th August 2017. By the last two days of the week, both methods demonstrated a clear decrease in risk. On 30th

August and 31st August 2017, over 70 % of neighborhoods fell in the 'very low' risk category in both methods, reflecting the efficacy of mitigating measures or the subsiding of flood intensity.

Overall, despite minor discrepancies, the IAHP and equal weighting methods showed a general agreement in risk categorization, and equal weight seemed to be more sensitive towards the detection of higher risk levels. The results emphasize the importance of selecting appropriate weighting methods in the risk assessment process.

3.5. Comparison with damage data

Damage data (including car insurance claims and property claims) resulting from the impacts caused by Hurricane Harvey, published by FEMA (2017), was used as a proxy to compare with our computed flood risks. Although the damage assessments are organized in daily map layers, they are cumulative from 25th August 2017. To compare the risk results with the damage map clearly, the damage data of the last day (31st August 2017) and the maximum flood risk map of this study (27th August 2017) were selected (see Fig. A.5 in Appendix A). The risk map was reclassified using the Natural Breaks Classification Method for this purpose.

From Fig. A.5, we can see that the geographical distribution of flood damage is consistent with the distribution of urban waterways, which is logical. Regions that are classified as having a significant risk of flooding, including those with very high, high, and medium levels of risk, have a higher density of reported damage. It is important to highlight that some neighborhoods (e.g., 9 and 17), despite being classified with very high flood risks, exhibit few reported instances of damage. This may be because these neighborhoods have a high density of urban forests, parks and lower residential density. Similarly, neighborhood 42, with a medium flood risk level, contains Houston's international airport.

It can be noticed that some areas with a low risk of flooding also have many instances of damage reports. The differences might be due to the daily hazard data used in this study. In real-world scenarios, there may be short periods where the flood risk escalated substantially, leading to extensive damage to infrastructures and vehicles. Therefore, where data is available, our research suggests using flood hazard data at finer temporal scales, such as minutes or hours, to calculate flood risks. Another point is that the damage data is mainly focused on car and property damage. However, the risk assessment in this study includes both the social and ecological systems, offering a more comprehensive overview. As such, the damage data can only provide some aspects of the overall flood risks. This underscores the need for a multi-dimensional approach to understanding and assessing flood risk.

4. Discussions and conclusions

Following a literature review, a SES urban flood risk assessment conceptual framework was developed, and an indicator list with 117 indicators was proposed. As a case study, we conducted a flood risk assessment for Houston during Hurricane Harvey by applying the urban SES conceptual framework. It is important to note that the proposed conceptual framework can provide a flexible tool which can be used for different urban contexts by adjusting indicators since the principle "one size fits all" cannot be applied to complex and dynamic realities. Consequently, the selection of indicators should be considered according to the specific urban context.

As a promising research trend in recent years in the context of urban planning and management, SES assessments in urban flood risk assessment are still rarely implemented. This study has modified an existing SES conceptual framework, introducing a variety of indicators. However, the number of indicators of social systems and ecosystems remains uneven. Therefore, the urban ecosystems in Houston cannot be fully represented. This could be problematic as several NBS projects have been implemented in Houston, and the local authority has acknowledged the mitigating effects of NBS (Yang and Li, 2013). Incorporating comprehensive indicators of urban ecosystems into flood risk assessments can provide valuable information to policymakers about the effectiveness of urban ecosystems and NBS projects. Hence, more efforts are needed in the future to truly consider the ecological indicators in urban flood risk assessment.

In alignment with the proposed conceptual framework and indicator list, this paper analyzed flood risks in Houston areas during Hurricane Harvey using two weighting methods. The differences in results show the importance of weighting method's selection in flood risk assessment process. A suitable weighting method should be considered carefully, taking into consideration the specific urban contexts and overarching objectives of the research.

The flood risk maps generated during Hurricane Harvey reflect the areas in Houston being impacted by flooding, illustrating those regions with higher levels of risk that are likely to experience more negative consequences. To strengthen the urban adaptive capacity and resilience, it is imperative that future mitigation efforts focus on these identified vulnerable areas within Houston. To better capture the flood risks, it is recommended that future studies employ flood hazard data characterized by finer temporal resolution, such as minute or hourly increments, thereby facilitating a more accurate assessment of flood risk.

The conclusions are summarized as follows:

a) The proposed conceptual framework and indicator list can be applied to other urban areas worldwide, with careful consideration of the specific context. The outcomes of such assessments can support informed decision-making, particularly in the development of DRR plans tailored for urban contexts.
b) The IAHP weighting results show that population density is the most significant factor influencing exposure. Population considered vulnerable (specifically, the population under 5 or above 65 years old, as well as disabled people) and the percentage of wetland loss emerge as important factors characterizing the vulnerability of Houston.
c) The results indicate that the western regions of Houston show very high flood risks, while the northeastern regions show high and medium flood risks. The central regions of Houston were comparatively subject to lower flood risks during Hurricane Harvey.
d) A comparative analysis between the IAHP and the equal weighting methods demonstrates that the latter calculates a higher risk score. The selection of the weighting method evidently plays a crucial role in the flood risk assessment process. Both weighting methods provided valuable insights into flood risks, with the equal weighting method simplifying the calculation process.

Overall, this study not only illustrates the potentially most flood-prone areas in Houston, but also reflects the implications of different weighting methods used in flood risk assessments. Therefore, we believe this study can provide helpful information for other researchers, decision-makers and local authorities for flood risk assessment and management.

Supplementary data to this article can be found online at https://doi.org/10.1016/j.scitotenv.2023.166891.

Declaration of competing interest

The authors declare that they have no known competing financial interests or personal relationships that could have appeared to influence the work reported in this paper.

Data availability

I have shared the link of my data sources in the Supplementary Material.

Acknowledgments

The contribution of Dianyu Feng was supported by the China Scholarship Council (201906200125) and University of Glasgow College of Social Sciences. We would like to thank all the experts involved in the online questionnaires for their expert advice regarding the indicator selection and weight assignment. We would also like to thank the editor and anonymous reviewers for their time and helpful comments, which helped improve the quality of the paper.

References

Anderson, C., Renaud, F., Hagenlocher, M., Day, J., 2021. Assessing multi-hazard vulnerability and dynamic coastal flood risk in the Mississippi Delta: the global delta risk index as a social-ecological systems approach. Water 13, 577. https://doi.org/10.3390/w13040577.

Balica, S., Douben, N., Wright, N., 2009. Flood vulnerability indices at varying spatial scales. Water Sci. Technol. J. Int. Assoc. Water Pollut. Res. 60, 2571–2580. https://doi.org/10.2166/wst.2009.183.

Balica, S.F., Wright, N.G., van der Meulen, F., 2012. A flood vulnerability index for coastal cities and its use in assessing climate change impacts. Nat. Hazards 64 (1), 73–105. https://doi.org/10.1007/s11069-012-0234-1.

Birkmann, J., Cardona, O.D., Carreño, M.L., Barbat, A.H., Pelling, M., Schneiderbauer, S., Kienberger, S., Keiler, M., Alexander, D., Zeil, P., Welle, T., 2013. Framing vulnerability, risk and societal responses: the MOVE framework. Nat. Hazards 67 (2), 193–211. https://doi.org/10.1007/s11069-013-0558-5.

Blake, E., Zelinsky, D., 2018. National Hurricane Center tropical cyclone report - Hurricane Harvey. https://www.nhc.noaa.gov/data/tcr/AL092017_Harvey.pdf.

Brakenridge, G.R., Kettner, A.J., 2023. DFO Flood Event 4510. Dartmouth Flood Observatory, University of Colorado, Boulder, Colorado, USA. https://floodobservatory.colorado.edu/Events/2017USA4510/2017USA4510.html.

Cangialosi, J.P., Latto, A.S., Berg, R., 2021. National Hurricane Center tropical cyclone report - Hurricane Irma. https://www.nhc.noaa.gov/data/tcr/AL112017_Irma.pdf.

Centre for Research on the Epidemiology of Disasters, 2023. 2022 Disasters in Numbers. CRED, Brussels. https://cred.be/sites/default/files/2022_EMDAT_report.pdf.

Chakraborty, S., Mukhopadhyay, S., 2019. Assessing flood risk using analytical hierarchy process (AHP) and geographical information system (GIS): application in Coochbehar district of West Bengal, India. Nat. Hazards 99 (1), 247–274. https://doi.org/10.1007/s11069-019-03737-7.

Chakraborty, J., Collins, T.W., Grineski, S.E., 2018. Exploring the environmental justice implications of Hurricane Harvey flooding in greater Houston, Texas. Am. J. Public Health 109 (2), 244–250. https://doi.org/10.2105/AJPH.2018.304846.

City of Houston, 2014. About Houston: facts and figures. https://www.houstontx.gov/abouthouston/houstonfacts.html.

Commission, E., & Innovation, D.-G. for R and, 2021. Evaluating the Impact of Nature-based Solutions: A Handbook for Practitioners. Publications Office of the European Union. https://doi.org/10.2777/244577.

Czajkowski, J., Villarini, G., Montgomery, M., Michel-Kerjan, E., Goska, R., 2017. Assessing current and future freshwater flood risk from North Atlantic tropical cyclones via insurance claims. Sci. Rep. 7 (1), 41609. https://doi.org/10.1038/srep41609.

Damm, M., 2010. Mapping Social-Ecological Vulnerability to Flooding. Universitäts-und Landesbibliothek Bonn (Doctoral dissertation).

Depietri, Yaella, McPhearson, T., 2017. Integrating the grey, green, and blue in cities: nature-based solutions for climate change adaptation and risk reduction. In: H, J, S., Nadja, B.A. Kabisch, Korn (Eds.), Nature-based Solutions to Climate Change Adaptation in Urban Areas: Linkages Between Science, Policy and Practice. Springer International Publishing, pp. 91–109. https://doi.org/10.1007/978-3-319-56091-5_6.

Eini, M., Kaboli, H.S., Rashidian, M., Hedayat, H., 2020. Hazard and vulnerability in urban flood risk mapping: machine learning techniques and considering the role of urban districts. Int. J. Disaster Risk Reduction 50 (March), 101687. https://doi.org/10.1016/j.ijdrr.2020.101687.

Elboshy, B., Kanae, S., Gamaleldin, M., Ayad, H., Osaragi, T., Elbarki, W., 2019. A framework for pluvial flood risk assessment in Alexandria considering the coping capacity. Environ. Syst. Decis. 39 (1), 77–94. https://doi.org/10.1007/s10669-018-9684-7.

Federal Emergency Management Agency, 2017. Historic disaster response to Hurricane Harvey in Texas, FEMA. https://www.fema.gov/press-release/20210318/historic-disaster-response-hurricane-harvey-texas (September).

Fletcher, T.D., Andrieu, H., Hamel, P., 2013. Understanding, management and modelling of urban hydrology and its consequences for receiving waters: a state of the art. Adv. Water Resour. 51, 261–279. https://doi.org/10.1016/j.advwatres.2012.09.001.

Hagenlocher, M., Renaud, F.G., Haas, S., Sebesvari, Z., 2018. Vulnerability and risk of deltaic social-ecological systems exposed to multiple hazards. Sci. Total Environ. 631–632, 71–80. https://doi.org/10.1016/j.scitotenv.2018.03.013.

Hanh Nguyen, H., Venohr, M., Gericke, A., Sundermann, A., Welti, E.A.R., Haase, P., 2023. Dynamics in impervious urban and non-urban areas and their effects on run-off, nutrient emissions, and macroinvertebrate communities. Landsc. Urban Plan. 231, 104639 https://doi.org/10.1016/j.landurbplan.2022.104639.

Herath, H.M.M., Wijesekera, N.T.S., 2019. A state-of-the-art review of flood risk assessment in urban area. IOP Conf. Ser. Earth Environ. Sci. 281 (1) https://doi.org/10.1088/1755-1315/281/1/012029.

Huang, Y., Tian, Z., Ke, Q., Liu, J., Irannezhad, M., Fan, D., Hou, M., Sun, L., 2020. Nature-based solutions for urban pluvial flood risk management. WIREs Water 7. https://doi.org/10.1002/wat2.1421.

Intergovernmental Panel on Climate Change, 2014. In: Edenhofer, O., Pichs-Madruga, R., Sokona, Y., Farahani, E., Kadner, S., Seyboth, K., Adler, A., Baum, I., Brunner, S., Eickemeier, P., Kriemann, B., Savolainen, J., Schlömer, S., von Stechow, C., Zwickel, T., Minx, J.C. (Eds.), Climate Change 2014: Mitigation of Climate Change. Contribution of Working Group III to the Fifth Assessment Report of the Intergovernmental Panel on Climate Change. Cambridge University Press, Cambridge, United Kingdom and New York, NY, USA.

Intergovernmental Panel on Climate Change, 2022. In: Pörtner, H.-O., Roberts, D.C., Tignor, M., Poloczanska, E.S., Mintenbeck, K., Alegría, A., Craig, M., Langsdorf, S., Löschke, S., Möller, V., Okem, A., Rama, B. (Eds.), Climate Change 2022: Impacts, Adaptation and Vulnerability. Contribution of Working Group II to the Sixth Assessment Report of the Intergovernmental Panel on Climate Change. Cambridge University Press, Cambridge, UK and New York, NY, USA. https://doi.org/10.1017/9781009325844 (3056 pp.).

Kablan, M.K.A., Dongo, K., Coulibaly, M., 2017. Assessment of social vulnerability to flood in urban Côte d'Ivoire using the MOVE framework. Water 9 (4). https://doi.org/10.3390/w9040292.

Kamat, R., 2019. Urban flood vulnerability assessment of Bhopal, M.P., India. Int. J. Civ. Eng. Technol. 10, 2956–2977.

Kandilioti, G., Makropoulos, C., 2012. Preliminary flood risk assessment: the case of Athens. Nat. Hazards 61 (2), 441–468. https://doi.org/10.1007/s11069-011-9930-5.

Knutson, T.R., Chung, M.v., Vecchi, G., Sun, J., Hsieh, T.-L., Smith, A.J.P., 2021. Climate Change is Probably Increasing the Intensity of Tropical Cyclones. https://doi.org/10.5281/ZENODO.4570334.

Li, F., Phoon, K.-K., Du, X., Zhang, M., 2013. Improved AHP method and its application in risk identification. J. Constr. Eng. Manag. 139, 312–320. https://doi.org/10.1061/(ASCE)CO.1943-7862.0000605.

Li, Z., Li, X., Wang, Y., Quiring, S.M., 2019. Impact of climate change on precipitation patterns in Houston, Texas, USA. Anthropocene 25, 100193. https://doi.org/10.1016/j.ancene.2019.100193.

Li, X., Fu, D., Nielsen-Gammon, J., Gangrade, S., Kao, S.-C., Chang, P., Morales Hernández, M., Voisin, N., Zhang, Z., Gao, H., 2023. Impacts of climate change on future hurricane induced rainfall and flooding in a coastal watershed: a case study on Hurricane Harvey. J. Hydrol. 616, 128774 https://doi.org/10.1016/j.jhydrol.2022.128774.

Liu, W., Chen, W., Peng, C., 2014. Assessing the effectiveness of green infrastructures on urban flooding reduction: a community scale study. Ecol. Model. 291, 6–14.

Lyu, H.-M., Xu, Y.-S., Cheng, W.-C., Arulrajah, A., 2018. Flooding hazards across southern China and prospective sustainability measures. Sustainability 10 (5), 1682.

Meyer, V., H, D., S, S., 2009. Flood risk assessment in European river basins—concept, methods, and challenges exemplified at the Mulde river. Integr. Environ. Assess. Manag. 5, 17–26.

Müller, A., 2013. Flood risks in a dynamic urban agglomeration: a conceptual and methodological assessment framework. Nat. Hazards 65 (3), 1931–1950. https://doi.org/10.1007/s11069-012-0453-5.

Narayan, S., Nicholls, R., Clarke, D., Hanson, S., 2012. Investigating the source–pathway–receptor–consequence framework for coastal flood system analyses. In: Innovative Coastal Zone Management: Sustainable Engineering for a Dynamic Coast, pp. 22–31. https://doi.org/10.1680/ICZM2012.57494.0003.

National Oceanic and Atmospheric Administration [NOAA], 2023. Office for Coastal Management. In: C-CAP Regional Land Cover. NOAA Office for Coastal Management, Charleston, SC. www.coast.noaa.gov/htdata/raster1/landcover/bulkdownload/30m_lc/.

Pasch, J.R., Penny, A.B., Berg, R., 2023. National Hurricane Center tropical cyclone report - Hurricane Maria. https://www.nhc.noaa.gov/data/tcr/AL152017_Maria.pdf.

Peng, Y., Welden, N., Renaud, F.G., 2023. A framework for integrating ecosystem services indicators into vulnerability and risk assessments of deltaic social-ecological systems. J. Environ. Manag. 326, 116682 https://doi.org/10.1016/j.jenvman.2022.116682.

Percival, S., Gaterell, M., Teeuw, R., 2019. Urban neighbourhood flood vulnerability and risk assessments at different diurnal levels. J. Flood Risk Manag. 12 (3), e12466 https://doi.org/10.1111/jfr3.12466.

Rana, I.A., Routray, J.K., 2018. Integrated methodology for flood risk assessment and application in urban communities of Pakistan. Nat. Hazards 91 (1), 239–266. https://doi.org/10.1007/s11069-017-3124-8.

Rincón, D., Khan, U.T., Armenakis, C., 2018. Flood risk mapping using GIS and multi-criteria analysis: a greater Toronto area case study. Geosciences 8 (8). https://doi.org/10.3390/geosciences8080275.

Sayers, P.B., Gouldby, B., Simm, J.D., Hawkes, P.J., Ramsbottom, D.M., Meadowcroft, I.C., Hall, J.W., 2002. Risk, performance and uncertainty in flood and coastal defence - a review. In: DEFRA/EA R&D Technical Report FD2302/TR1 (HR Wallingford Report SR587) January.

Schanze, J., 2006. Flood Risk Management—A Basic Framework. Springer.

Scheuer, S., Haase, D., Meyer, V., 2011. Exploring multicriteria flood vulnerability by integrating economic, social and ecological dimensions of flood risk and coping capacity: from a starting point view towards an end point view of vulnerability. Nat. Hazards 58 (2), 731–751. https://doi.org/10.1007/s11069-010-9666-7.

Sebesvari, Z., Renaud, F., Haas, S., Tessler, Z., Hagenlocher, M., Kloos, J., Szabo, S., Tejedor, A., Kuenzer, C., 2016. A review of vulnerability indicators for deltaic social–ecological systems. Sustain. Sci. 11 https://doi.org/10.1007/s11625-016-0366-4.

Shah, M.A.R., Renaud, F.G., Anderson, C.C., Wild, A., Domeneghetti, A., Polderman, A., Votsis, A., Pulvirenti, B., Basu, B., Thomson, C., Panga, D., Pouta, E., Toth, E., Pilla, F., Sahani, J., Ommer, J., El Zohbi, J., Munro, K., Stefanopoulou, M., Zixuan, W., 2020. A review of hydro-meteorological hazard, vulnerability, and risk assessment frameworks and indicators in the context of nature-based solutions. Int. J. Disaster Risk Reduction 50, 101728. https://doi.org/10.1016/J.IJDRR.2020.101728.

Tabari, H., 2020. Climate change impact on flood and extreme precipitation increases with water availability. Sci. Rep. 10 (1), 13768. https://doi.org/10.1038/s41598-020-70816-2.

Tellman, B., Sullivan, J.A., Kuhn, C., Kettner, A.J., Doyle, C.S., Brakenridge, G.R., Erickson, T.A., Slayback, D.A., 2021. Satellite imaging reveals increased proportion of population exposed to floods. Nature 596 (7870), 80–86. https://doi.org/10.1038/s41586-021-03695-w.

United Nations, 2015. Transforming our world: the 2030 agenda for sustainable development. https://sustainabledevelopment.un.org/content/documents/21252030%20Agenda%20for%20Sustainable%20Development%20web.pdf.

United Nations Office for Disaster Risk Reduction, 2015. Sendai framework for disaster risk reduction 2015-2030. https://www.unisdr.org/we/inform/publications/43291.

United Nations Office for Disaster Risk Reduction, 2019. Global assessment report on disaster risk reduction. https://gar.undrr.org/sites/default/files/reports/2019-05/full_gar_report.pdf.

United States Geological Survey, 2011. National Elevation Dataset. USGS, USA. https://data.tnris.org/collection?c=49c7fa9b-ab48-4c17-8f19-27253f7cfd08#4.98/31.43/-100.

Vlad, M.I., Nedelcu, I., 2011. Assessing the flood risk in urban environment using disaster risk management specific indicators. In: Gi4DM 2011 - GeoInformation for Disaster Management, pp. 21–25.

Waghwala, R., Agnihotri, P., 2019. Assessing the impact index of urbanization index on urban flood risk. Int. J. Recent Technol. Eng. 8 https://doi.org/10.35940/ijrte.B1571.078219.

Wasko, C., Sharma, A., 2017. Global assessment of flood and storm extremes with increased temperatures. Sci. Rep. 7 (1), 7945. https://doi.org/10.1038/s41598-017-08481-1.

World Bank, 2023. Urban development. https://www.worldbank.org/en/topic/urbandevelopment/overview.

Yan, B., Li, S., Wang, J., Ge, Z., Zhang, L., 2016. Socio-economic vulnerability of the megacity of Shanghai (China) to sea-level rise and associated storm surges. Reg. Environ. Chang. 16 (5), 1443–1456. https://doi.org/10.1007/s10113-015-0878-y.

Yang, B., Li, S., 2013. Green infrastructure design for stormwater runoff and water quality: empirical evidence from large watershed-scale community developments. Water 5 (4), 2038–2057. https://doi.org/10.3390/w5042038 (MDPI AG).

Yeganeh, N., Sabri, S., 2014. Flood vulnerability assessment in Iskandar Malaysia using multi-criteria evaluation and fuzzy logic. Res. J. Appl. Sci. Eng. Technol. 8, 1794–1806. https://doi.org/10.19026/rjaset.8.1167.

Yildirim, E., Demir, I., 2022. Agricultural flood vulnerability assessment and risk quantification in Iowa. Sci. Total Environ. 826, 154165 https://doi.org/10.1016/j.scitotenv.2022.154165.

Yilmaz, A., Rashetnia, S., Muttil, N., 2015. Developing a flood vulnerability index for a case study area in Melbourne. In: Conference: 36th Hydrology and Water Resources Symposium: The Art and Science of Water.

Zhang, W., Villarini, G., Vecchi, G.A., Smith, J.A., 2018. Urbanization exacerbated the rainfall and flooding caused by hurricane Harvey in Houston. Nature 563 (7731), 384–388. https://doi.org/10.1038/s41586-018-0676-z.

Zhang, D., Shi, X., Xu, H., Jing, Q., Pan, X., Liu, T., Wang, H., Hou, H., 2020. A GIS-based spatial multi-index model for flood risk assessment in the Yangtze River Basin, China. Environ. Impact Assess. Rev. 83, 106397 https://doi.org/10.1016/J.EIAR.2020.106397.

Zimmermann, E., Bracalenti, L., Piacentini, R., Inostroza, L., 2016. Urban flood risk reduction by increasing green areas for adaptation to climate change. Procedia Eng. 161, 2241–2246. https://doi.org/10.1016/j.proeng.2016.08.822.